A Unified Spectral Method for FPDEs with Two-sided Derivatives; part I: A Fast Solver

Mehdi Samiee[1,2], Mohsen Zayernouri[1,2,*] and Mark M. Meerschaert[3]

[1] *Department of Computational Mathematics, Science, and Engineering, Michigan State University, 428 S.Shaw Lane East Lansing MI 48824, USA*

[2] *Department of Mechanical Engineering, Michigan State University, 428 S.Shaw Lane East Lansing MI 48824, USA*

[3] *Department of Statistics and Probability, Michigan State University, 619 Red Cedar Road Wells Hall East Lansing MI 48824, USA*

Abstract

We develop a unified Petrov-Galerkin spectral method for a class of fractional partial differential equations with two-sided derivatives and constant coefficients of the form ${}_0\mathcal{D}_t^{2\tau} u + \sum_{i=1}^{d} [c_{l_i}\, {}_{a_i}\mathcal{D}_{x_i}^{2\mu_i} u + c_{r_i}\, {}_{x_i}\mathcal{D}_{b_i}^{2\mu_i} u] + \gamma\ u = \sum_{j=1}^{d} [\kappa_{l_j}\, {}_{a_j}\mathcal{D}_{x_j}^{2\nu_j} u + \kappa_{r_j}\, {}_{x_j}\mathcal{D}_{b_j}^{2\nu_j} u] + f$, where $2\tau \in (0,2)$, $2\mu_j \in (0,1)$ and $2\nu_j \in (1,2)$, in a $(1+d)$-dimensional *space-time* hypercube, $d = 1, 2, 3, \cdots$, subject to homogeneous Dirichlet initial/boundary conditions. We employ the eigenfunctions of the fractional Sturm-Liouville eigen-problems of the first kind in [1], called *Jacobi poly-fractonomial*s, as temporal bases, and the eigen-functions of the boundary-value problem of the second kind as temporal test functions. Next, we construct our spatial basis/test functions using Legendre polynomials, yielding mass matrices being independent of the spatial fractional orders ($\mu_j,\ \nu_j,\ j = 1, 2, \cdots, d$). Furthermore, we formulate a novel unified fast linear solver for the resulting high-dimensional linear system based on the solution of generalized eigen-problem of spatial mass matrices with respect to the corresponding stiffness matrices, hence, making the complexity of the problem optimal, i.e., $\mathcal{O}(N^{d+2})$. We carry out several numerical test cases to examine the CPU time and convergence rate of the method. The corresponding stability and error analysis of the Petrov-Galerkin method are carried out in [2].

*Corresponding author. Fax: +1 517 353 1750. E-mail address: zayern@msu.edu

Preprint submitted to JCP *October 24, 2016*

Keywords: Anomalous transport, high-dimensional FPDEs, diffusion-to-wave dynamics, Jacobi poly-fractonomial, Legendre polynomials, unified fast solver, spectral convergence

1. Introduction

Fractional calculus seamlessly generalizes the notion of standard integer-order calculus to its fractional-order counterpart, leading to a broader class of mathematical models, namely fractional ordinary differential equations (FODEs) and fractional partial differential equations (FPDEs) [3, 4, 5, 6, 7]. Such non-local models appear as tractable mathematical tools to describe anomalous transport, which manifests in memory-effects, non-local interactions, power-law distributions, sharp peaks, and self-similar structures [8, 4, 9, 10]. Although anomalous, such phenomena are observed in a range of applications e.g., bioengineering [11, 12, 13, 14], turbulent flows [15, 16, 17, 18, 19], porous media [20, 21, 22], viscoelastic materials [23].

Due to their history dependence and non-local character, the discretization of such problems becomes computationally challenging. Numerical methods, developed to discretize FPDEs, can be categorized in two major classes: i) local methods, e.g., finite difference method (FDM), finite volume method (FVM), and finite element method (FEM), and ii) global methods, e.g., single and multi-domain spectral methods (SM).

Local schemes have been studied extensively in the literature. Lubich introduced the discretized fractional calculus within the spirit of FDM [24]. Sugimoto employed a FDM scheme for approximating fractional Burger's equation [25, 26]. Meerschaert and Tadjeran [27] developed finite difference approximations to solve one-dimensional advection-dispersion equations with variable coefficients on a finite domain. Tadjeran and Meerschaert [28] employed a practical alternating directions implicit (ADI) method to solve a class of fractional partial differential equations with variable coefficients in bounded domain. Hejazi et al., [29] developed a finite-volume method utilizing fractionally shifted grunwald formula for the fractional derivatives for space-fractional advection-dispersion equation on a finite domain. To solve the two-dimensional two-sided space-fractional convection diffusion equation, Chen and Deng [30] proposed a practical alternating directions implicit method. Zeng et al., [31] constructed a finite element method and a multistep method for unconditionally stable time-integration of sub-diffusion problem. In addition, Zhao et al., developed second-order FDM for the variable-order FPDEs in [32]. Li et al., [33] proposed an implicit finite difference scheme for solving the generalized time-fractional Burger's equation. Recently, Feng et al., [34] proposed a second-order Crank-Nicolson scheme to approximate the Riesz space-fractional advection-dispersion equations (FADE). Moreover, two compact non-ADI FDMs have been proposed for the high-dimensional time-fractional sub-diffusion equation by Zeng et al., [35]. Recently, Zayernouri and Matzavinos [36] have developed an explicit fractional adams/Bashforth/Moulton and implicit fractional Adams-Moulton finite difference methods, applicable to high-order time-integration of nonlinear FPDEs and amenable for formulating implicit/explicit (IMEX) splitting methods.

Regarding global methods, Sugimoto [25, 26] used Fourier SM in a fractional Burger's equation. Shen and Wang [37] constructed a set of Fourier-like basis functions for Legendre-Galerkin method for non-periodic boundary value problems and proposed a new space-time spectral method. Sweilam et al., [38] considered Chebyshev Pseudo-spectral method for solving one-dimensional FADE, where the fractional derivative is described in Caputo sense. Chen et al., [39] developed an approach for high-order time integration within multi-domain setting for time-fractional diffusion equations. Mokhtary developed a fully discrete Galerkin method to numerically approximate initial value fractional integro-differential equations [40].

Moreover, Zayernouri and Karniadakis [1, 41] introduced a new family of basis/test functions, called *(tempered)Jacobi poly-fractonomials*, known as the explicit eigenfunctions of (tempered) fractional Strum-Liouville problems in bounded domains of the first and second kind. Following this new spectral theory, they have developed a number of single- and multi-domain spectral methods [42, 43, 44, 45, 46]. Recently, Dehghan et al. [47], employed a Galerkin finite element and interpolating element free Galerkin methods for full discretization of the fractional diffusion-wave equation. They [48] also introduced a full discretization of time-fractional diffusion and wave equations using meshless Galerkin method based on radial basis functions. Zaho et al., [49] developed a spectral method for the tempered fractional diffusion equations (TFDEs) using the generalized Jacobian functio [50]. Mao and Shen [51] developed Galerkin spectral methods for solving multi-dimensional fractional elliptic equations with variable coefficients.

The main contribution of the present work is to construct a unified Petrov-Galerkin spectral method and a unified fast solver for the weak form of linear

FPDEs with constant coefficients in (1+d) dimensional *space-time* hypercube of the form

$$
\begin{aligned}
{}_0\mathcal{D}_t^{2\tau} u + \sum_{i=1}^{d} [c_{l_i}\, {}_{a_i}\mathcal{D}_{x_i}^{2\mu_i} u + c_{r_i}\, {}_{x_i}\mathcal{D}_{b_i}^{2\mu_i} u] \;&=\; \sum_{j=1}^{d} [\kappa_{l_j}\, {}_{a_j}\mathcal{D}_{x_j}^{2\nu_j} u + \kappa_{r_j}\, {}_{x_j}\mathcal{D}_{b_j}^{2\nu_j} u] \\
&\quad -\gamma\; u + f, \qquad (1)
\end{aligned}
$$

where $2\mu_i, \in [0,\, 1]$, $2\nu_i, \in [1,\, 2]$, and $2\tau, \in [0,\, 2]$ subject to Dirichlet initial and boundary conditions, where $i = 1,\, 2,\, ...,\, d$. Compared to FPDEs considered in [45], here, we include an additional advection term that allows (1) to also include the fractional advection-dispersion equation (FADE). We employ the Jacobi poly-fractonomials as temporal basis/test functions and Legendre polynomials as spatial basis/test functions. We develop a new general fast linear solver based on the eigenpairs of the corresponding temporal mass and the spatial matrices with respect to the temporal stiffness and spatial mass matrices, respectively. In [2], we perform the corresponding discrete stability and error analyses of the PG method along with several verifying numerical tests.

The outline of this paper is as follows: in section 2, we introduce some preliminary results from fractional calculus. In section 3, we present the mathematical formulation of the spectral method in a (d+1) dimensional space, which leads to the generalized Lyapunov equations. In section 4, we develop a unified fast linear solver and obtain the closed-form solution in terms of the genralized eigenvalues and eigenvectors of the corresponding mass and stiffness matrices. In section 5, the performance of the PG method is examined via several numerical simulations for low-to- high dimensional problems with smooth and non-smooth solutions.

2. Preliminaries on Fractional Calculus

Here, we obtain some basic definitions from fractional calculus [4, 45]. Denoted by ${}_a\mathcal{D}_x^{\nu} g(x)$ is the left-sided Reimann-Liouville fractional derivative of order ν in which $g(x) \in C^n[a, b]$, defined as:

$$
{}^{RL}_{\;a}\mathcal{D}_x^{\nu} g(x) = \frac{1}{\Gamma(n-\nu)} \frac{d^n}{dx^n} \int_a^x \frac{g(s)}{(x-s)^{\nu+1-n}}\; ds, \quad x \in [a, b], \qquad (2)
$$

where Γ represents the Euler gamma function. The corresponding right-sided Reimann-Liouville fractional derivative of order ν, ${}_{x}\mathcal{D}_{b}^{\nu} g(x)$, is given by

$$ {}^{RL}_{\;\;x}\mathcal{D}_{b}^{\nu} g(x) = \frac{1}{\Gamma(n-\nu)} (-1)^n \frac{d^n}{dx^n} \int_{x}^{b} \frac{g(s)}{(s-x)^{\nu+1-n}} \, ds, \quad x \in [a,b]. \tag{3} $$

In (2) and (3), as $\nu \to n$, the fractional derivatives tend to the standard n-th order derivative with respect to x. We recall from [52] that the following link between the Reimann-Liouville and Caputo fractional derivatives, where

$$ {}^{Rl}_{\;\;a}\mathcal{D}_{x}^{\mu} f(x) \; = \; \frac{f(a)}{\Gamma(1-\mu)(x-a)^{\mu}} \; + \; {}^{C}_{a}\mathcal{D}_{x}^{\mu} f(x) \tag{4} $$

$$ {}^{Rl}_{\;\;x}\mathcal{D}_{b}^{\mu} f(x) \; = \; \frac{f(b)}{\Gamma(1-\mu)(b-x)^{\mu}} \; + \; {}^{C}_{x}\mathcal{D}_{b}^{\mu} f(x), \tag{5} $$

where

$$ {}^{C}_{a}\mathcal{D}_{x}^{\mu} f(x) \; = \; \frac{1}{\Gamma(n-\nu)} \int_{a}^{x} \frac{g^{(n)}(s)}{(x-s)^{\nu+1-n}} \, ds, \quad x \in [a,b], \tag{6} $$

$$ {}^{C}_{x}\mathcal{D}_{b}^{\mu} f(x) \; = \; \frac{(-1)^n}{\Gamma(n-\nu)} \int_{x}^{b} \frac{g^{(n)}(s)}{(x-s)^{\nu+1-n}} \, ds, \quad x \in [a,b], \tag{7} $$

In (4) and (5), ${}^{RL}_{\;\;a}\mathcal{D}_{x}^{\nu} g(x) = {}^{C}_{a}\mathcal{D}_{x}^{\nu} g(x) = {}_{a}\mathcal{D}_{x}^{\nu} g(x)$ when homogeneous Dirichlet initial and boundary conditions are enforced.

To analytically obtain the fractional differentiation of our basis function, we employ the following relations [1] as:

$$ {}^{RL}_{\;\,-1}\mathcal{I}_{x}^{\mu} \{(1+x)^{\beta} P_{n}^{\alpha,\beta}(x)\} = \frac{\Gamma(n+\beta+1)}{\Gamma(n+\beta+\mu+1)} \, (1+x)^{\beta+\mu} P_{n}^{\alpha-\mu,\beta+\mu}(x), \tag{8} $$

and

$$ {}^{RL}_{\;\;x}\mathcal{I}_{1}^{\mu} \{(1-x)^{\alpha} P_{n}^{\alpha,\beta}(x)\} = \frac{\Gamma(n+\alpha+1)}{\Gamma(n+\alpha+\mu+1)} \, (1-x)^{\alpha+\mu} P_{n}^{\alpha+\mu,\beta-\mu}(x), \tag{9} $$

where $0 < \mu < 1$, $\alpha > -1$, $\beta > -1$ and $P_{n}^{\alpha,\beta}(x)$ denote the standard Jacobi Polynomials of order n and parameters α and β. It is worth mentioning that

$$ {}^{RL}_{\;\;a}\mathcal{I}_{x}^{\mu} \{f(x)\} = \frac{1}{\Gamma(\mu)} \int_{a}^{x} \frac{f(s)}{(x-s)^{1-\mu}} \, ds, \quad x \in [a,b], $$

$$ {}^{RL}_{\;\;x}\mathcal{I}_{b}^{\mu} \{f(x)\} = \frac{1}{\Gamma(\mu)} \int_{x}^{b} \frac{f(s)}{(s-x)^{1-\mu}} \, ds, \quad x \in [a,b]. $$

By substituting $\alpha = +\mu$ and $\beta = -\mu$, we can simplify equations (8) and (9), thereby we have:

$$ {}^{RL}_{-1}\mathcal{I}^{\mu}_{x}\{(1+x)^{-\mu}P_n^{\mu,-\mu}(x)\} = \frac{\Gamma(n-\mu+1)}{\Gamma(n+1)}P_n(x), \quad x \in [-1,1] \tag{10} $$

and

$$ {}^{RL}_{x}\mathcal{I}^{\mu}_{1}\{(1-x)^{\mu}P_n^{-\mu,\mu}(x)\} = \frac{\Gamma(n-\mu+1)}{\Gamma(n+1)}P_n(x), \quad x \in [-1,1]. \tag{11} $$

Accordingly, we have the fractional derivative of Legendre polynomial by differentiating equations (8) and (9) as

$$ {}_{-1}\mathcal{D}^{\mu}_{x}P_n(x) = \frac{\Gamma(n+1)}{\Gamma(n-\mu+1)}P_n^{\mu,-\mu}(x)\,(1+x)^{-\mu} \tag{12} $$

and

$$ {}_{x}\mathcal{D}^{\mu}_{1}P_n(x) = \frac{\Gamma(n+1)}{\Gamma(n-\mu+1)}P_n^{-\mu,\mu}(x)\,(1-x)^{-\mu}, \tag{13} $$

where $P_n(x) = P_n^{0,0}(x)$ represents Legendre polynomial of degree n.

3. Mathematical Framework

Let $u : \mathbb{R}^{d+1} \to \mathbb{R}$ for some positive integer d and $\Omega = [0,T] \times [a_1,b_1] \times [a_2,b_2] \times \cdots \times [a_d,b_d]$, where

$$ \begin{aligned} {}_{0}\mathcal{D}^{2\tau}_{t}u \quad &+ \quad \sum_{i=1}^{d}\left[c_{l_i}\ {}_{a_i}\mathcal{D}^{2\mu_i}_{x_i}u + c_{r_i}\ {}_{x_i}\mathcal{D}^{2\mu_i}_{b_i}u\right] \\ &- \quad \sum_{j=1}^{d}\left[\kappa_{l_j}\ {}_{a_j}\mathcal{D}^{2\nu_j}_{x_j}u + \kappa_{r_j}\ {}_{x_j}\mathcal{D}^{2\nu_j}_{b_j}u\right] + \gamma\ u = f, \end{aligned} \tag{14} $$

where, $\gamma, c_{l_i}, c_{r_i}, \kappa_{l_i}$, and κ_{r_i} are all constant. $2\mu_j \in (0,1)$, $2\nu_j \in (1,2)$, and $2\tau \in (0,2)$, for $j = 1,2,\cdots,d$. This equation is subject to the following Dirichlet initial and boundary conditions as:

$$ \begin{aligned} u|_{t=0} &= 0, \quad \tau \in (0,1/2), \\ u|_{t=0} &= \frac{\partial u}{\partial t}|_{t=0} = 0, \quad \tau \in (1/2,1), \\ u|_{x_j=a_j} = u|_{x_j=b_j} &= 0, \quad \nu_j \in (1/2,1), \quad j = 1,2,\cdots,d. \end{aligned} $$

We define the solution space U as

$$U := \Big\{ u : \Omega \to \mathbb{R} \,|\, u \in C(\Omega),\ \|u\|_U < \infty,\ \ u|_{t=0} = u|_{x_j=a_j} = u|_{x_j=b_j} = 0 \Big\}$$

when $\nu_j \in (1/2, 1)$ and

$$\begin{aligned} \|u\|_U \;\; &= \;\; \Big\{ \| \, {}_0\mathcal{D}_t^{\tau} \, (u) \|_{L^2}^2 + \sum_{j=1}^{d} \Big[\| \, {}_{a_j}\mathcal{D}_{x_j}^{\mu_j} \, (u) \|_{L^2}^2 + \| \, {}_{x_j}\mathcal{D}_{b_j}^{\mu_j} \, (u) \|_{L^2}^2 \Big] \\ &+ \sum_{i=1}^{d} \Big[\| \, {}_{a_i}\mathcal{D}_{x_i}^{\nu_i} \, (u) \|_{L^2}^2 + \| \, {}_{x_i}\mathcal{D}_{b_i}^{\nu_i} \, (u) \|_{L^2}^2 \Big] + \|u\|_{L^2}^2 \Big\}^{1/2} \end{aligned} \tag{15}$$

The test space V is defined correspondingly as

$$V := \Big\{ v : \Omega \to \mathbb{R} \,|\, \|v\|_V < \infty,\ v|_{t=T} = v|_{x_j=b_j} = 0 \Big\} \tag{16}$$

when $\nu_j \in (1/2, 1)$ and $\mu_i \in (0, 1/2)$, in which

$$\begin{aligned} \|v\|_V \;\; &= \;\; \Big\{ \| \, {}_t\mathcal{D}_T^{\tau} \, (v) \|_{L^2}^2 + \sum_{j=1}^{d} \Big[\| \, {}_{x_j}\mathcal{D}_{b_j}^{\mu_j} \, (v) \|_{L^2}^2 + \| \, {}_{a_j}\mathcal{D}_{x_j}^{\mu_j} \, (v) \|_{L^2}^2 \Big] \\ &+ \sum_{i=1}^{d} \Big[\| \, {}_{x_i}\mathcal{D}_{b_i}^{\nu_i} \, (v) \|_{L^2}^2 + \| \, {}_{a_i}\mathcal{D}_{x_i}^{\nu_i} \, (v) \|_{L^2}^2 \Big] + \|v\|_{L^2}^2 \Big\}^{1/2}. \end{aligned} \tag{17}$$

U and V are Hilbert spaces [53].

3.1. ***Stochastic Interpretation of the FPDEs***

Following [54], we provide a brief stochastic interpretation of the FPDEs in (14) that further sheds light on the well-posedness of the problem from the perspective of probability theory. Let suppose that in (14), $f \equiv 0$ and $\gamma = 0$ and $0 < 2\tau < 1$ and that $a_i = -\infty$ and $b_i = +\infty$ for $i = 1, 2, \cdots$. Then (14) governs [54] a time-changed Lévy process $X(E_t)$ on $\mathbb{R}^d$ whose Fourier transform is $\mathbb{E}[e^{-ik \cdot X(t)}] = e^{t\psi(k)}$ with the Fourier symbol

$$\psi(k) = -\sum_{n=1}^{d} [c_{l_n}(ik_n)^{2\mu_n} + c_{r_n}(-ik_n)^{2\mu_n}] + \sum_{m=1}^{d} [\kappa_{l_m}(-ik_m)^{2\nu_m} + \kappa_{r_m}(ik_m)^{2\nu_m}]. \tag{18}$$

Recall that in one dimension the Lévy process $Y(t)$ with Fourier Transform $\mathbb{E}[e^{-ikY(t)}] = e^{t\psi_0(k)}$ where $\psi_0(k) = pD(ik)^\alpha + qD(-ik)^\alpha$ for $D > 0$ and $1 < \alpha \leq 2$, $p \geq 0$, $q \geq 0$, and $p + q = 1$ is a stable Lévy process with index α and skewness $p - q$ [4, 54].

In brief, fractional advection-dispersion equation on unbounded domain is represented by a solution involves an inverse stable subordinator time-changed, resulting in an non-Markovian process. You can find complete details in [4].

Regarding a computational domain, Chen et al [55] developed a solution for the case of equation (14) where $f \equiv 0$ and $\gamma = 0$ and $0 < 2\tau < 1$ and all $a_m = a_n > -\infty$ and $b_m = b_n < \infty$, with zero Dirichlet boundary conditions. It follows from [54] that

$$Lu(x) = cu'(x) + \kappa_l \, {}_a\mathcal{D}_x^{2\nu} u(x) + \kappa_r \, {}_x\mathcal{D}_b^{2\nu} u(x) \tag{19}$$

is the generator of the killed semigroup on the bounded domain $\Omega = (a, b)$ which is also the point source to (14). In other words, starting with the point source initial condition $u(x, 0) = \delta(x)$, the solution to (14) with the restrictions discussed in [4, 55] is the PDF of a *killed non-Markovian* process.

3.2. ***Petrov-Galerkin Method***

We construct a Petrov-Galerkin spectral method for $u \in U$, satisfying the corresponding weak form of (14) as

$$\begin{aligned}
({}_0\mathcal{D}_t^{\tau}\, u, {}_t\mathcal{D}_T^{\tau}\, v)_\Omega \;&+\; \sum_{i=1}^{d} \Big[c_{l_i}({}_{a_i}\mathcal{D}_{x_i}^{\mu_i}\, u,\; {}_{x_i}\mathcal{D}_{b_i}^{\mu_i}\, v)_\Omega + c_{r_i}({}_{a_i}\mathcal{D}_{x_i}^{\mu_i}\, v,\; {}_{x_i}\mathcal{D}_{b_i}^{\mu_i}\, u)_\Omega\Big] \\
&-\; \sum_{j=1}^{d} [k_{l_j}({}_{a_j}\mathcal{D}_{x_j}^{\nu_j}\, u,\; {}_{x_j}\mathcal{D}_{b_j}^{\nu_j}\, v)_\Omega + k_{r_j}({}_{a_j}\mathcal{D}_{x_j}^{\nu_j}\, v,\; {}_{x_j}\mathcal{D}_{b_j}^{\nu_j}\, u)_\Omega] \\
&+\; \gamma(u, v)_\Omega = (f, v)_\Omega, \quad \forall v \in V,
\end{aligned} \tag{20}$$

where $(\cdot,\cdot)_\Omega$ represents the usual L^2-product. Next, let $a : U \times V \to \mathbb{R}$ be a bilinear form, defined as

$$
\begin{aligned}
a(u,v) \;=\; & ({}_0\mathcal{D}_t^{\tau}\, u, {}_t\mathcal{D}_T^{\tau}\, v)_\Omega \\
& + \sum_{i=1}^{d} \Big[c_{l_i} ({}_{a_i}\mathcal{D}_{x_i}^{\mu_i}\, u,\; {}_{x_i}\mathcal{D}_{b_i}^{\mu_i}\, v)_\Omega + c_{r_i} ({}_{x_i}\mathcal{D}_{a_i}^{\mu_i}\, u,\; {}_{a_i}\mathcal{D}_{x_i}^{\mu_i}\, v)_\Omega \Big] \\
& + \sum_{j=1}^{d} \Big[\kappa_{l_j} ({}_{a_j}\mathcal{D}_{x_j}^{\nu_j}\, u,\; {}_{x_j}\mathcal{D}_{b_j}^{\nu_j}\, v)_\Omega + \kappa_{r_j} ({}_{x_j}\mathcal{D}_{b_j}^{\nu_j}\, u,\; {}_{a_j}\mathcal{D}_{x_j}^{\nu_j}\, v)_\Omega \Big] \\
& + \gamma(u,v)_\Omega. \qquad (21)
\end{aligned}
$$

Now, the problem reads as: find $u \in U$ such that

$$a(u,v) = (f,v), \quad \forall v \in V, \qquad (22)$$

where $a(u,v)$ is a continuous bilinear form. Next, we choose proper subspaces of U and V as finite dimensional U_N and V_N with $\dim(U_N) = \dim(V_N) = N$. Now, the discrete problem is to find $u_N \in U_N$ such that

$$a(u_N, v_N) = (f, v_N), \quad \forall v_N \in V_N. \qquad (23)$$

By representing u_N as a linear combination of points/elements in U_N i.e., the corresponding $(1+d)$-dimensional space-time basis functions, the finite-dimensional problem (23) leads to a linear system known as *Lyapunov* system. For instance, when $d = 1$, we obtain the corresponding Lyapunov equation in the space-time domain $[0,T] \times [a_1, b_1]$ as

$$
\begin{aligned}
S_\tau\, \mathcal{U}\, M_1^T \;+\; & c_{l_1} M_\tau\, \mathcal{U}\, S_{\mu_1,l}^T + c_{r_1} M_\tau\, \mathcal{U}\, S_{\mu_1,r}^T \\
-\; & \kappa_{l_1} M_\tau\, \mathcal{U}\, S_{\nu_1,l}^T - \kappa_{r_1} M_\tau\, \mathcal{U}\, S_{\nu_1,r}^T = F, \qquad (24)
\end{aligned}
$$

where all are defined in 3.5.

To find the general form of Lyapunov equation, we can define S^{Tot} as

$$\kappa_{l_1} S_{\nu_1,l} + \kappa_{r_1} S_{\nu_1,r} + c_{l_1} S_{\mu_1,l} + c_{r_1} S_{\mu_1,r} = S_1^{Tot}. \qquad (25)$$

Considering equation (25), we obtain the (1+1)-D space-time Lyapunov system as

$$S_\tau\, \mathcal{U}\, M_1^T + M_\tau\, \mathcal{U}\, S_1^{Tot^T} = F.$$

We present a new class of basis and test functions yielding *symmetric* stiffness matrices. Moreover, we compute exactly the corresponding mass matrices, which are either *symmetric* and *pentadiagonal*. In the following, we extensively study the properties of the aforementioned matrices, allowing us to formulate a general fast linear solver for (42).

3.3. Space of Basis Functions (U_N)

We construct our basis for the spatial discretization employing the Legendre polynomials defined as

$$\phi_m(\,\xi\,) = \sigma_m \left(P_{m+1}(\xi) \, - \, P_{m-1}(\xi)\right), \quad m = 1, 2, \cdots \quad \textit{and} \;\; \xi \in [-1, 1], \tag{26}$$

where $\sigma_m = 2 + (-1)^m$. The definition reflects the fact that for $\mu \leq 1/2$ and $1/2 \;\leq \nu \leq 1$, then both boundary conditions needs to be presented. Naturally, for the temporal basis functions only initial conditions are prescribed and the basis function for the temporal discretization is constructed based on the univariate poly-fractonomials [1] as

$$\psi^{\tau}_n(\eta) = \sigma_n (1+\eta)^{\tau} \; P^{-\tau\,,\,\tau}_{n-1}(\eta), \quad n = 1, 2, \cdots \quad \textit{and} \;\; \eta \in [-1, 1], \tag{27}$$

for $n \geq 1$. With the notation established, we define the space-time trial space to be

$$U_N = span\Big\{ \Big(\psi^{\tau}_n \circ \eta\Big)(t) \prod_{j=1}^{d} \Big(\phi_{m_j} \circ \xi_j\Big)(x_j) \; : n = 1, \ldots, \mathcal{N}, \, m_j = 1, \ldots, \mathcal{M}_j \Big\}, \tag{28}$$

where $\eta(t) = 2t/T - 1$ and $\xi_j(s) = 2\frac{s-a_j}{b_j-a_j} - 1$.

3.4. Space of Test Functions (V_N)

We construct our *spatial* test functions using Legendre polynomial as well as the basis function in our Galerkin method as

$$\Phi^{\mu}_k(\xi) = \widetilde{\sigma}_k \, \left(P_{k+1}(\xi) \, - \, P_{k-1}(\xi)\right), \quad k = 1, 2, \cdots \quad \textit{and} \;\; \xi \in [-1, 1], \tag{29}$$

where $\widetilde{\sigma}_k = 2\,(-1)^k + 1$. Next, we define the *temporal* test functions using the univariate poly-fractonomials

$$\Psi^{\tau}_r(\eta) = \widetilde{\sigma}_r \, (1-\eta)^{\tau} \; P^{\tau\,,\,-\tau}_{r-1}(\eta), \quad r = 1, 2, \cdots \quad \textit{and} \;\; \eta \in [-1, 1], \tag{30}$$

and we construct the corresponding space-time test space as

$$V_N = span\Big\{ \Big(\Psi^{\tau}_r \circ \eta\Big)(t) \prod_{j=1}^{d} \Big(\Phi_{k_j} \circ \xi_j\Big)(x_j) \, : r = 1, \dots, \mathcal{N}, \; k_j = 1, \dots, \mathcal{M}_j \Big\}. \tag{31}$$

Remark 3.1. The choices of σ_m in (26) and (27), also $\widetilde{\sigma}_k$ in (29) and (30), result in the spatial/temporal mass and stiffness matrices being *symmetric*, which are discussed in Theorems 3.2, 3.3, and 3.4 in more details.

3.5. ***Implementation of PG Spectral Method***

We now seek the solution to (14) in terms of a linear combination of elements in the space U_N of the form

$$u_N(x,t) = \sum_{n=1}^{\mathcal{N}} \sum_{m_1=1}^{\mathcal{M}_1} \cdots \sum_{m_d=1}^{\mathcal{M}_d} \hat{u}_{n,m_1,\cdots,m_d} \Big[\psi^{\tau}_n(t) \prod_{j=1}^{d} \phi_{m_j}(x_j) \Big] \tag{32}$$

in Ω. We enforce the corresponding residual

$$\begin{aligned} R_N(t, x_1, \cdots, x_d) \;\; = \;\; & {}_0\mathcal{D}_t^{2\tau} u_N + \sum_{i=1}^{d} [c_{l_i} \; {}_{a_i}\mathcal{D}_{x_i}^{2\mu_i} u_N + c_{r_i} \; {}_{x_i}\mathcal{D}_{b_i}^{2\mu_i} u_N] \\ - \;\; & \sum_{j=1}^{d} [\kappa_{l_j} \;\; {}_{a_j}\mathcal{D}_{x_j}^{2\nu_j} u_N + \kappa_{r_j} \;\; {}_{x_j}\mathcal{D}_{b_j}^{2\nu_j} u_N] \\ + \;\; & \gamma \, u_N - f \end{aligned} \tag{33}$$

to be L^2-orthogonal to $v_N \in V_N$, which leads to the finite-dimensional variational weak form in (23). Specifically, by choosing $v_N = \Psi^{\tau}_r(t) \prod_{j=1}^{d} \Phi_{k_j}(x_j)$, when $r = 1, \ldots, \mathcal{N}$ and $k_j = 1, \ldots, \mathcal{M}_j$, $j = 1, 2, \cdots, d$, we have

$$
\begin{aligned}
\sum_{n=1}^{\mathcal{N}} \sum_{m_1=1}^{\mathcal{M}_1} \cdots \sum_{m_d=1}^{\mathcal{M}_d} \hat{u}_{n,m_1,\cdots,m_d} \Bigg(& \{S_\tau\}_{r,n} \{M_1\}_{k_1,m_1} \cdots \{M_d\}_{k_d,m_d} \\
+ & \sum_{i=1}^{d} [c_{l_i} \{M_\tau\}_{r,n} \{M_1\}_{k_1,m_1} \cdots \{S_{\nu_i,l}\}_{k_i,m_i} \cdots \{M_d\}_{k_d,m_d} \\
+ & c_{r_i} \{M_\tau\}_{r,n} \{M_1\}_{k_1,m_1} \cdots \{S_{\nu_i,r}\}_{k_i,m_i} \cdots \{M_d\}_{k_d,m_d}] \\
- & \sum_{j=1}^{d} \Big[\kappa_{l_j} \{M_\tau\}_{r,n} \{M_1\}_{k_1,m_1} \cdots \{S_{\nu_j,l}\}_{k_j,m_j} \cdots \{M_d\}_{k_d,m_d} \\
+ & \kappa_{r_j} \{M_\tau\}_{r,n} \{M_1\}_{k_1,m_1} \cdots \{S_{\nu_j,r}\}_{k_j,m_j} \cdots \{M_d\}_{k_d,m_d}\Big] \\
+ & \gamma \{M_\tau\}_{r,n} \{M_1\}_{k_1,m_1} \cdots \{M_d\}_{k_d,m_d} \Bigg) \\
= & F_{r,k_1,\cdots,k_d},
\end{aligned}
$$

where S_τ and M_τ denote, respectively, the temporal stiffness and mass matrices whose entries are defined as

$$\{S_\tau\}_{r,n} = \int_0^T {}_0\mathcal{D}_t^\tau \Big(\psi_n^\tau \circ \eta \Big)(t) \, {}_t\mathcal{D}_T^\tau \Big(\Psi_r^\tau \circ \eta \Big)(t) \, dt,$$

and

$$\{M_\tau\}_{r,n} = \int_0^T \Big(\Psi_r^\tau \circ \eta \Big)(t) \Big(\psi_n^\tau \circ \eta \Big)(t) \, dt.$$

Moreover, S_{μ_j} and M_{μ_j}, $j = 1, 2, \cdots, d$, are the corresponding spatial stiffness and mass matrices where the left-sided and right-sided entries of the spatial stiffness matrices are obtained as

$$\{S_{\mu_j,l}\}_{k_j,m_j} = \int_{a_j}^{b_j} {}_{a_j}\mathcal{D}_{x_j}^{\mu_j} \Big(\phi_{m_j}^{\mu_j} \circ \xi_j \Big)(x_j) \; {}_{x_j}\mathcal{D}_{b_j}^{\mu_j} \Big(\Phi_{k_j}^{\mu_j} \circ \xi_j \Big)(x_j) \, dx_j = \{S_{\mu_j}\}_{k_j,m_j},$$

$$\{S_{\mu_j,r}\}_{k_j,m_j} = \int_{a_j}^{b_j} {}_{x_j}\mathcal{D}_{b_j}^{\mu_j} \Big(\phi_{m_j}^{\mu_j} \circ \xi_j \Big)(x_j) \; {}_{a_j}\mathcal{D}_{x_j}^{\mu_j} \Big(\Phi_{k_j}^{\mu_j} \circ \xi_j \Big)(x_j) \, dx_j = \{S_{\mu_j}\}_{k_j,m_j}^T,$$

and the corresponding entries of the spatial mass matrix are given by

$$\{M_j\}_{k_j,m_j} = \int_{a_j}^{b_j} \Big(\Phi_{k_j} \circ \xi_j \Big)(x_j) \Big(\phi_{m_j} \circ \xi_j \Big)(x_j) \, dx_j.$$

Moreover, the components of the load vector are computed as

$$F_{r,k_1,\cdots,k_d} \quad = \quad \int_{\Omega} f(t, x_1, \cdots, x_d)\Big(\Psi_r^{\tau} \circ \eta\Big)(t) \prod_{j=1}^{d} \Big(\Phi_{k_j} \circ \xi_j\Big)(x_j)\, d\Omega. \quad (34)$$

The linear system (34) can be exhibited as the following general Lyapunov equation

$$\begin{aligned} \Big(\quad & S_\tau \otimes M_1 \otimes M_2 \cdots \otimes M_d \qquad (35) \\ + \quad & \sum_{i=1}^{d} c_{l_i} M_\tau \otimes M_1 \otimes \cdots \otimes S_{\mu_i,l} \otimes M_{i+1} \cdots \otimes M_d \\ + \quad & \sum_{i=1}^{d} c_{r_i} M_\tau \otimes M_1 \otimes \cdots \otimes S_{\mu_i,r} \otimes M_{i+1} \cdots \otimes M_d \\ - \quad & \sum_{j=1}^{d} \kappa_{l_j} M_\tau \otimes M_1 \otimes \cdots \otimes S_{\nu_j,l} \otimes M_{j+1} \cdots \otimes M_d \\ - \quad & \sum_{j=1}^{d} \kappa_{r_j} M_\tau \otimes M_1 \otimes \cdots \otimes S_{\nu_j,r} \otimes M_{j+1} \cdots \otimes M_d \\ + \quad & \gamma\ M_\tau \otimes M_1 \otimes M_2 \cdots \otimes M_d \Big) \mathcal{U} = F. \end{aligned}$$

Let

$$c_{l_i} \times S_{\mu_i,l} + c_{r_i} \times S_{\mu_i,r} - \kappa_{l_i} \times S_{\nu_i} - \kappa_{r_i} \times S_{\nu_i,r} = S^{Tot}. \qquad (36)$$

Considering the fact that all the aforementioned stiffness and mass matrices are *symmetric*, $S_{\mu_i,l}$, $S_{\mu_i,r}$, $S_{\nu_i,l}$, and $S_{\nu_i,r}$ can be replaced by S^{Tot} which remains symmetric. Therefore,

$$\begin{aligned} & \Big(S_\tau \otimes M_1 \otimes M_2 \cdots \otimes M_d \qquad (37) \\ & + \sum_{i=1}^{d} [\ M_\tau \otimes M_1 \otimes \cdots \otimes M_{j-1} \otimes S_i^{Tot} \otimes M_{i+1} \cdots \otimes M_d\ ] \\ & + \gamma\ M_\tau \otimes M_1 \otimes M_2 \cdots \otimes M_d \Big) \mathcal{U} = F, \end{aligned}$$

in which $\otimes$ represents the Kronecker product, F denotes the multi-dimensional load matrix whose entries are given in (34), and $\mathcal{U}$ denotes the corresponding multi-dimensional matrix of unknown coefficients with entries $\hat{u}_{n,m_1,\cdots,m_d}$.

In the Theorems 3.2, 3.3, and 3.4, we study the properties of the aforementioned matrices. Besides, we present efficient ways of deriving the spatial mass matrices and the temporal stiffness matrices analytically and exact computation of the temporal mass and the spatial stiffness matrices through proper quadrature rules.

Theorem 3.2. *The temporal stiffness matrix S_τ corresponding to the time-fractional order $\tau \in (0,1)$ is a diagonal $\mathcal{N} \times \mathcal{N}$ matrix, whose entries are obtained as*

$$\{S_\tau\}_{r,n} = \widetilde{\sigma}_r \, \sigma_n \frac{\Gamma(n+\tau)}{\Gamma(n)} \, \frac{\Gamma(r+\tau)}{\Gamma(r)} \Big(\frac{2}{T}\Big)^{2\tau-1} \, \frac{2}{2n-1} \, \delta_{r,n}, \quad r,n = 1,2,\cdots,\mathcal{N}.$$

Moreover, the he entries of temporal mass matrices M_τ can be computed exactly by employing a Gauss-Lobatto-Jacobi (GLJ) rule with respect to the weight function $(1-\eta)^\tau(1+\eta)^\tau$, $\eta \in [-1,1]$, where $\alpha = \tau/2$. Moreover, M_τ is symmetric.

Proof. See [45]. □

Theorem 3.3. *The spatial mass matrix M is a penta-diagonal $\mathcal{M} \times \mathcal{M}$ matrix, whose entries are explicitly given as*

$$M_{k,r} \;=\; \widetilde{\sigma}_k \, \sigma_r \, [\frac{2}{2k+3}\delta_{k,r} - \frac{2}{2k+3}\delta_{k+1,r-1} - \frac{2}{2k-3}\delta_{k-1,r+1} + \frac{2}{2k-3}\delta_{k-1,r-1}. \quad (38)$$

Proof. The (k, r)*th*-entry of the spatial mass matrix is given by

$$M_{k,r} = \int_a^b \phi_r \circ \xi(x) \, \Phi_k \circ \xi(x) \, dx = \big(\tfrac{b-a}{2}\big) \int_{-1}^1 \phi_r(\xi)\Phi_k(\xi) \, d\xi, \qquad (39)$$

where $\xi = 2\frac{x-a}{b-a} - 1$ and $\xi \in (-1,\, 1)$. Substituting the spatial basis/test functions, we have

$$M_{k,r} = \big(\tfrac{b-a}{2}\big) \, \widetilde{\sigma}_k \, \sigma_r \, \big[\, \widetilde{M}_{k,r} - \widetilde{M}_{k+1,r-1} - \widetilde{M}_{k-1,r+1} + \widetilde{M}_{k,r}\big], \qquad (40)$$

in which

$$\widetilde{M}_{i,j} = \int_{-1}^1 P_i(\xi) \, P_j(\xi) \, d\xi \qquad = \frac{2}{2i+1}\delta_{ij}. \qquad (41)$$

Therefore, we have

$$M_{k,r} \;=\; \big(\frac{b-a}{2}\big) \, \widetilde{\sigma}_k \, \sigma_r \, [\frac{2}{2k+3}\delta_{k,r} - \frac{2}{2k+3}\delta_{k+1,r-1} - \frac{2}{2k-3}\delta_{k-1,r+1} + \frac{2}{2k-3}\delta_{k,r}]$$

as a pentadiagonal matrix. Moreover,

$$\begin{aligned} M_{r,k} &= (\frac{b-a}{2})\,\widetilde{\sigma}_r\,\sigma_k\,[\frac{2}{2r+3}\delta_{r,k} - \frac{2}{2r+3}\delta_{r+1,k-1} - \frac{2}{2r-3}\delta_{r-1,k+1} + \frac{2}{2r-3}\delta_{r,k}] \\ &= M_{k,r} \end{aligned}$$

□

Theorem 3.4. *The total spatial stiffness matrix S^{Tot} is symmetric and its entries can be exactly computed as:*

$$c_{l_i} \times S_{\mu_i,l} + c_{r_i} \times S_{\mu_i,r} - \kappa_{l_i} \times S_{\nu_i,l} - \kappa_{r_i} \times S_{\nu_i,r} = S^{Tot}. \tag{42}$$

where $i = 1, 2, \cdots, d$.

Proof. Regarding the definition of stiffness matrix, we have

$$\begin{aligned} \{S_{\mu_i,l}\}_{r,n} &= \int_{a_i}^{b_i} {}_{a_i}\mathcal{D}_{x_i}^{\mu_i}\Big(\,\phi_n(x_i)\Big)\,{}_{x_i}\mathcal{D}_{b_i}^{\mu_i}\Big(\Phi_r(x_i)\Big)\,dx_i, \\ &= (\frac{b_i-a_i}{2})^{-2\mu_i+1}\int_{-1}^{1} {}_{-1}\mathcal{D}_{\xi_i}^{\mu_i}\Big(\,P_{n+1}-P_{n-1}\Big)\,{}_{\xi_i}\mathcal{D}_{1}^{\mu_i}\Big(\,P_{k+1}-P_{k-1}\Big)\,d\xi_i \\ &= (\frac{b_i-a_i}{2})^{-2\mu_i+1}\,\widetilde{\sigma}_r\,\sigma_n\,\Big[\,\widetilde{S}^{\mu_i}_{r+1,n+1} - \widetilde{S}^{\mu_i}_{r+1,n-1} - \widetilde{S}^{\mu_i}_{r-1,n+1} + \widetilde{S}^{\mu_i}_{r-1,n-1}\Big], \end{aligned} \tag{43}$$

where

$$\widetilde{S}^{\mu_i}_{r,n} = \int_{-1}^{1} {}_{-1}\mathcal{D}_{\xi_i}^{\mu_i}\Big(\,P_n(\xi_i)\Big)\,{}_{\xi_i}\mathcal{D}_{1}^{\mu_i}\Big(\,P_r(\xi_i)\Big)\,d\xi_i$$
$$= \int_{-1}^{1} \tfrac{\Gamma(r+1)}{\Gamma(r-\mu_i+1)}\,\tfrac{\Gamma(n+1)}{\Gamma(n-\mu_i+1)}\,(1+\xi_i)^{-\mu_i}(1-\xi_i)^{-\mu_i}\,P_r^{-\mu_i,\mu_i}\,P_n^{\mu_i,-\mu_i}d\xi_i.$$

Furthermore,

$$\begin{aligned} \{S_{\mu_i,r}\}_{r,n} &= \int_{a_i}^{b_i} {}_{a_i}\mathcal{D}_{x_i}^{\mu_i}\Big(\,\Phi_r(x_i)\Big)\,{}_{x_i}\mathcal{D}_{b_i}^{\mu_i}\Big(\phi_n(x_i)\Big)\,dx_i, \\ &= \int_{a_i}^{b_i} {}_{a_i}\mathcal{D}_{x_i}^{\mu_i}\Big(\,\phi_n(x_i)\Big)\,{}_{x_i}\mathcal{D}_{b_i}^{\mu_i}\Big(\Phi_r(x_i)\Big)\,dx_i, \\ &= \{S_{\mu_i,l}\}_{r,n} = \{S_{\mu_i}\}_{r,n} \end{aligned} \tag{44}$$

Similar to (44), we get $\{S_{\nu_i,l}\}_{r,n} = \{S_{\nu_i,r}\}_{r,n} = \{S_{\nu_i}\}_{r,n}$; as a result,

$$(\kappa_{l_i} + \kappa_{r_i})\,S_{\nu_i} + (c_{l_i} + c_{r_i})\,S_{\mu_i} = S_i^{Tot}. \tag{45}$$

$\widetilde{S}^{\mu_i}_{r,n}$ can be computed accurately using Guass-Jacobi quadrature rule as

$$\widetilde{S}^{\mu}_{r,n} = \frac{\Gamma(r+1)}{\Gamma(r-\mu_i+1)}\frac{\Gamma(n+1)}{\Gamma(n-\mu_i+1)}\sum_{q=1}^{Q} w_q\, P^{-\mu_i,\mu_i}_r(\xi_q)P^{\mu_i,-\mu_i}_n(\xi_q), \quad (46)$$

in which $\mathcal{Q} \geq \mathcal{N}+2$ represents the minimum number of GJ quadrature points $\{\xi_q\}_{q=1}^{\mathcal{Q}}$, associated with the weigh function $(1-\xi)^{-\mu_i}(1+\xi)^{-\mu_i}$, for *exact* quadrature, and $\{w_q\}_{q=1}^{Q}$ are the corresponding quadrature weights. Employing the property of the Jacobi polynomials where $P^{\alpha,\beta}_n(-x_i) = (-1)^n P^{\beta,\alpha}_n(x_i)$, we can re-express $\widetilde{S}^{\mu_i}_{r,n}$ as $(-1)^{(r+n)}\,\widetilde{S}^{\mu_i}_{n,r}$. Accordingly,

$$\begin{aligned}\{S_{\mu_i}\}_{r,n} = \left(\tfrac{b_i-a_i}{2}\right)^{-2\mu_i+1}\widetilde{\sigma}_r\,\sigma_n\,\big[&(-1)^{(n+r+2)}\,\widetilde{S}^{\mu_i}_{n+1,r+1} - (-1)^{(n+r)}\,\widetilde{S}^{\mu_i}_{n+1,r-1}\\ &-(-1)^{(n+r)}\,\widetilde{S}^{\mu_i}_{n-1,r+1} + (-1)^{(n+r-2)}\,\widetilde{S}^{\mu_i}_{n-1,r-1}\big]\\ = \widetilde{\sigma}_r\,\sigma_n\,(-1)^{(n+r)}\,\big[&\widetilde{S}^{\mu}_{n+1,r+1} - \widetilde{S}^{\mu_i}_{n+1,r-1} - \widetilde{S}^{\mu_i}_{n-1,r+1} + \widetilde{S}^{\mu_i}_{n-1,r-1}\big]. \quad (47)\end{aligned}$$

According to (47),

$$\{S_{\mu_i}\}_{r,n} = \{S_{\mu_i}\}_{n,r} \times \frac{\widetilde{\sigma}_r\,\sigma_n}{\widetilde{\sigma}_n\,\sigma_r}(-1)^{(n+r)}. \quad (48)$$

In fact, $\widetilde{\sigma}_r$ and σ_n are chosen such that $(-1)^{(n+r)}$ is canceled; hence it can be easily concluded that the stiffness matrix $S^{\mu_i}_{n,r}$, $S^{\nu_i}_{n,r}$ and thereby $S^{Tot}_{n,r}$ as the sum of two symmetric matrices are symmetric. □

4. Unified Fast FPDE Solver

We formulate a closed-form solution for the Lyapunov system (37) in terms of the generalised eigensolutions that can be computed very efficiently, leading to the following unified fast solver for the development of Petrov-Galerkin spectral method.

Theorem 4.1. *Let $\{\vec{e}^{\,\mu_j}, \lambda_{m_j}\}_{m_j=1}^{\mathcal{M}_j}$ be the set of general eigen-solutions of the spatial stiffness matrix S^{Tot}_j with respect to the mass matrix M_j. Moreover, let $\{\vec{e}^{\,\tau}_n, \lambda^{\tau}_n\}_{n=1}^{\mathcal{N}}$ be the set of general eigen-solutions of the temporal mass matrix M_τ with respect to the stiffness matrix S_τ.*

(I) if $d>1$, then the multi-dimensional matrix of unknown coefficients $\mathcal{U}$ is explicitly obtained as

$$\mathcal{U} = \sum_{n=1}^{\mathcal{N}}\sum_{m_1=1}^{\mathcal{M}_1}\cdots\sum_{m_d=1}^{\mathcal{M}_d}\kappa_{n,m_1,\cdots,m_d}\;\vec{e}^{\,\tau}_n \otimes \vec{e}_{m_1} \otimes\cdots\otimes \vec{e}_{m_d}, \quad (49)$$

where $\kappa_{n,m_1,\cdots,m_d}$ are given by

$$\kappa_{n,m_1,\cdots,m_d} = \frac{(\vec{e}_n^{\,\tau}\, \vec{e}_{m_1} \cdots \vec{e}_{m_d})F}{\Big[(\vec{e}_n^{\,\tau^T} S_\tau \vec{e}_n^{\,\tau}) \prod_{j=1}^{d} (\vec{e}_{m_j}^{\,T} M_j \vec{e}_{m_j})\Big] \Lambda_{n,m_1,\cdots,m_d}}, \tag{50}$$

in which the numerator represents the standard multi-dimensional inner product, and $\Lambda_{n,m_1,\cdots,m_d}$ are obtained in terms of the eigenvalues of all mass matrices as

$$\Lambda_{n,m_1,\cdots,m_d} = \Big[(1+\gamma\ \lambda_n^\tau) + \lambda_n^\tau \textstyle\sum_{j=1}^{d} (\lambda_{m_j})\Big].$$

(II) If $d=1$, then the two-dimensional matrix of the unknown solution $\mathcal{U}$ is obtained as

$$\mathcal{U} = \sum_{n=\lceil 2\tau \rceil}^{\mathcal{N}} \sum_{m_1=1}^{\mathcal{M}_1} \kappa_{n,m_1}\ \vec{e}_n^{\,\tau}\ \vec{e}_{m_1}^{\,T},$$

where κ_{n,m_1} is explicitly obtained as

$$\kappa_{n,m_1} = \frac{\vec{e}_n^{\,\tau^T} F\, \vec{e}_{m_1}}{(\vec{e}_n^{\,\tau^T} S_\tau \vec{e}_n^{\,\tau})(\vec{e}_{m_1}^{\,T} M_1 \vec{e}_{m_1})\Big[(1+\gamma\ \lambda_n^\tau) +\ \lambda_n^\tau\, \lambda_{m_1}\Big]}.$$

Proof. Let us consider the following generalised eigenvalue problems as

$$S_j^{Tot}\, \vec{e}_{m_j} = \lambda_{m_j}^j\, M_j\, \vec{e}_{m_j}, \quad m_j = 1,\cdots,\mathcal{M}_j, \quad j=1,2,\cdots,d, \tag{51}$$

and

$$M_\tau\, \vec{e}_n^{\,\tau} = \lambda_n^\tau\, S_\tau\, \vec{e}_n^{\,\tau}, \quad n = 1,2,\cdots,\mathcal{N}. \tag{52}$$

Having the spatial and temporal eigenvectors determined in equations (52) and (51), we can represent the unknown coefficient matrix $\mathcal{U}$ in (32) in terms of the aforementioned eigenvectors as

$$\mathcal{U} = \sum_{n=1}^{\mathcal{N}} \sum_{m_1=1}^{\mathcal{M}_1} \cdots \sum_{m_d=1}^{\mathcal{M}_d} \kappa_{n,m_1,\cdots,m_d}\ \vec{e}_n^{\,\tau} \otimes \vec{e}_{m_1} \otimes \cdots \otimes \vec{e}_{m_d}, \tag{53}$$

where $\kappa_{n,m_1,\cdots,m_d}$ are obtained as follows. First, we take the multi-dimensional inner product of $\vec{e}_q^{\,\tau}\, \vec{e}_{p_1} \cdots \vec{e}_{p_d}$ on both sides of the Lyapunov equation (37) as

$$
\begin{aligned}
&(\, \vec{e}_q^{\,\tau}\, \vec{e}_{p_1}\, \vec{e}_{p_2} \cdots \vec{e}_{p_d}) \Big[\, S_\tau \otimes M_1 \otimes \cdots \otimes M_d \\
&+ \textstyle\sum_{j=1}^{d} \left[M_\tau \otimes M_1 \otimes \cdots \otimes M_{j-1} \otimes S_j^{Tot} \otimes M_{j+1} \cdots \otimes M_d\right] \\
&+\gamma\ M_\tau \otimes M_1 \otimes \cdots \otimes M_d \Big] \mathcal{U} = (\, \vec{e}_q^{\,\tau}\, \vec{e}_{p_1} \cdots \vec{e}_{p_d}) F.
\end{aligned}
$$

Then, by replacing (51) and (52) into (50) and re-arranging the terms, we get

$$
\begin{aligned}
\sum_{n=1}^{\mathcal{N}} \sum_{m_1=1}^{\mathcal{M}_1} \cdots \sum_{m_d=d}^{\mathcal{M}_d} \kappa_{n,m_1,\cdots,m_d} \times \Big(\ & \vec{e}_q^{\,\tau^T} S_\tau \vec{e}_n^{\,\tau}\ \ \vec{e}_{p_1}^T M_1 \vec{e}_{m_1}\ \cdots\ \vec{e}_{p_d}^T M_d\, \vec{e}_{m_d} \\
+ \ & \sum_{j=1}^{d} \vec{e}_q^{\,\tau^T} M_\tau \vec{e}_n^{\,\tau}\ \ \vec{e}_{p_1}^T M_1 \vec{e}_{m_1}\ \cdots\ \vec{e}_{p_j}^T S_j^{Tot} \vec{e}_{m_j}\ \ \vec{e}_{p_{j+1}}^T M_{j+1} \vec{e}_{m_{j+1}}\ \cdots \vec{e}_{p_d}^T M_d \vec{e}_{m_d} \\
+ \ & \gamma\ \vec{e}_q^{\,\tau^T} M_\tau \vec{e}_n^{\,\tau}\ \ \vec{e}_{p_1}^T M_{\mu_1} \vec{e}_{m_1}\ \ \vec{e}_{p_2}^T M_2 \vec{e}_{m_2}\ \cdots\ \vec{e}_{p_d}^T M_d \vec{e}_{m_d} \Big) \\
= \ & (\, \vec{e}_q^{\,\tau}\, \vec{e}_{p_1}\, \vec{e}_{p_2} \cdots \vec{e}_{p_d}) F.
\end{aligned}
$$

Recalling that $S_j^{Tot} \vec{e}_{m_j} = (\lambda_{m_j} M_j\, \vec{e}_{m_j})$ and $M_\tau\, \vec{e}_n^{\,\tau} = (\lambda_n^\tau\, S_\tau\, \vec{e}_n^{\,\tau})$, we have

$$
\begin{aligned}
\sum_{n=1}^{\mathcal{N}} \sum_{m_1=1}^{\mathcal{M}_1} \cdots \sum_{m_d=1}^{\mathcal{M}_d} \kappa_{n,m_1,\cdots,m_d} \Big(\ & \vec{e}_q^{\,\tau^T} S_\tau \vec{e}_n^{\,\tau}\, \vec{e}_{p_1}^T M_1 \vec{e}_{m_1}\, \vec{e}_{p_2}^T M_2 \vec{e}_{m_2} \cdots \vec{e}_{p_d}^T M_d \vec{e}_{m_d}) \\
+ \ & \sum_{j=1}^{d} \vec{e}_q^{\,\tau^T} (\lambda_n^\tau\, S_\tau\, \vec{e}_n^{\,\tau})\, \vec{e}_{p_1} M_1 \vec{e}_{m_1} \cdots \vec{e}_{p_j}^T (\lambda_{m_j}^j M_j \vec{e}_{m_j}) \vec{e}_{p_{j+1}}^T M_{j+1} \vec{e}_{m_{j+1}} \cdots \vec{e}_{p_d}^T M_d \vec{e}_{m_d} \\
+ \ & \gamma\ \vec{e}_q^{\,\tau^T} (\lambda_n^\tau\, S_\tau\, \vec{e}_n^{\,\tau})\, \vec{e}_{p_1}^T M_1 \vec{e}_{m_1}\, \vec{e}_{p_2}^T M_2 \vec{e}_{m_2}\ \cdots\ \vec{e}_{p_d}^T M_d \vec{e}_{m_d} \Big) \\
= \ & (\, \vec{e}_q^{\,\tau}\, \vec{e}_{p_1}\, \vec{e}_{p_2} \cdots \vec{e}_{p_d}) F.
\end{aligned}
$$

Therefore,

$$
\kappa_{n,m_1,\cdots,m_d} = \frac{(\, \vec{e}_n^{\,\tau}\, \vec{e}_{m_1} \cdots \vec{e}_{m_d}) F}{\left[(\vec{e}_n^{\,\tau^T} S_\tau \vec{e}_n^{\,\tau}) \prod_{j=1}^{d} (\vec{e}_{m_j}^T M_j \vec{e}_{m_j})\right] \times \left[(1 + \gamma\ \lambda_n^\tau) + \lambda_n^\tau \sum_{j=1}^{d} (\lambda_{m_j})\right]}.
$$

Then, we have

$$
\begin{aligned}
&\textstyle\sum_{n=\lceil 2\tau \rceil}^{\mathcal{N}}\ \sum_{m_1=1}^{\mathcal{M}_1} \cdots \sum_{m_d=1}^{\mathcal{M}_d} \kappa_{n,m_1,\cdots,m_d} (\vec{e}_q^{\,\tau^T} S_\tau \vec{e}_n^{\,\tau})(\vec{e}_{p_1}^T M_1 \vec{e}_{m_1}) \cdots (\vec{e}_{p_d}^T M_d \vec{e}_{m_d}) \\
&\qquad \times \Big[(1 + \gamma\ \lambda_n^\tau) + \lambda_n^\tau \textstyle\sum_{j=1}^{d} (\lambda_{m_j})\Big] = (\, \vec{e}_q^{\,\tau}\, \vec{e}_{p_1}\, \vec{e}_{p_2} \cdots \vec{e}_{p_d}) F.
\end{aligned}
$$

On account of the fact that the spatial Mass M_j and temporal stiffness matrices S_τ are diagonal (see Theorems 3.3 and 3.2), we have $(\vec{e}_q^{\,\tau^T} S_\tau \vec{e}_n^{\,\tau}) = 0$ if $q \neq n$, and also $(\vec{e}_{p_j}^{\,T} M_j \vec{e}_{m_j}) = 0$ if $p_j \neq m_j$, which completes the proof for the case $d > 1$.

Following similar steps for the two-dimensional problem, it is easy to see that if $d = 1$, the relationship for κ can be derived as

$$\kappa_{q,p_1} = \frac{\vec{e}_q^{\,\tau^T} F \, \vec{e}_{p_1}}{(\vec{e}_q^{\,\tau^T} S_\tau \vec{e}_q^{\,\tau})(\vec{e}_{p_1}^{\,T} M_1 \vec{e}_{p_1})\Big[(1 + \gamma \; \lambda_n^\tau) + \; \lambda_n^\tau \, \lambda_{m_1}\Big]}. \tag{54}$$

In 4.1, we present a computational method for the fast solver which reduces the computational cost significantly. □

4.1. *Computational Considerations*

Employing the fast solver in $(1+d)$ dimensional problem $d \geq 1$ can reduce the dominant computational cost of the eigensolver, which is $\mathcal{O}(N^{2(1+d)})$. This approach becomes more efficient in higher dimensional problems. There are two steps, which are associated with the fast solver:

Step (i): computation of $\kappa_{n,m_1,m_2,\ldots,m_d}$ in (54),

Step (ii): constructing $\mathcal{U}$ in (53).

To compute $\kappa_{n,m_1,m_2,\ldots,m_d}$, we need to find the numerator as

$$(\vec{e}_q^{\,\tau} \, \vec{e}_{p_1}^{\,1} \cdots \, \vec{e}_{p_d}^{\,d}) F = \sum_{i=1}^{\mathcal{N}} \sum_{s_1=1}^{\mathcal{M}_1} \cdots \sum_{s_d=1}^{\mathcal{M}_d} \{\vec{e}_q^{\,\tau}\}_i \, \{\vec{e}_{p_1}^{\,1}\}_{s_1} \cdots \, \{\vec{e}_{p_d}^{\,d}\}_{s_d} \{F\}_{i,s_1,\cdots,s_d}, \tag{55}$$

which leads to a computational complexity $\mathcal{O}(N^{2(1+d)})$. Employing the sum-factorization, the numerator can be written as

$$(\vec{e}_q^{\,\tau} \, \vec{e}_{p_1} \cdots \, \vec{e}_{p_d}) F \;\; = \;\; \sum_{i=1}^{\mathcal{N}} \{\vec{e}_q^{\,\tau}\}_i \sum_{s_1=1}^{\mathcal{M}_1} \{\vec{e}_{p_1}\}_{s_1} \;\; \cdots \;\; \sum_{s_{d-1}=1}^{\mathcal{M}_{d-1}} \{\vec{e}_{p_{d-1}}\}_{s_{d-1}} \sum_{s_d=1}^{\mathcal{M}_d} \{\vec{e}_{p_d}\}_{s_d} \{F\}_{i,s_1,\cdots,s_d}, \tag{56}$$

in which the inner-most sum is obtained as

$$\mathcal{F}^{d}_{i,s_1,\cdots,s_{d-1},p_d} = \sum_{s_d=1}^{\mathcal{M}_d} \{\vec{e}^{\,d}_{p_d}\}_{s_d} \{F\}_{i,s_1,\cdots,s_d}, \tag{57}$$

and similarly, we can write the second one as

$$\mathcal{F}^{d-1}_{i,s_1,\cdots,s_{d-2},p_{d-1},p_d} = \sum_{s_{d-1}=1}^{\mathcal{M}_{d-1}} \{\vec{e}^{\,d-1}_{p_{d-1}}\}_{s_{d-1}} \mathcal{F}^{d}_{i,s_1,\cdots,s_{d-1},p_d}. \tag{58}$$

Finally, we get

$$\mathcal{F}^{1}_{i,p_1,\cdots,p_d} = \sum_{s_1=1}^{\mathcal{M}_1} \{\vec{e}^{\,1}_{p_1}\}_{s_1} \mathcal{F}^{2}_{i,p_1,p_2,\cdots,p_d}. \tag{59}$$

We observe that the computational cost can be reduced to $\mathcal{O}(N^{2+d})$. A similar sum-factorization technique can be applied to step (ii).

5. Numerical Tests

We now examine the unified PG spectral method and the corresponding unified fast solver (53) and (54) for (14) in the context of several numerical test cases in order to investigate the spectral/exponential rate of convergence in addition to the computational efficiency of the scheme. The corresponding force term f in (14) is obtained in Appendix for the following test cases, listed as:

Test case (I): (smooth solutions with finite regularity) we consider the following exact solution to perform the temporal *p-refinement* as

$$u^{exact} = t^{p_1} \times ((1+x)^{p_2} - \epsilon(1+x)^{p_3}), \tag{60}$$

where $p_1 = 7\frac{2}{3}$, $p_2 = 6\frac{1}{3}$, $p_3 = 6\frac{2}{7}$ and $t \in [0,\, 1]$ and $x \in [-1,\, 1]$.

Test case (II): (spatially smooth function) we consider

$$u^{exact} = t^{p_1} \times sin[n\pi\,(1+x)], \tag{61}$$

where $n = 1$ and $p_1 = 6\frac{1}{3}$, for the exponential *p-refinement*.

Test case (III): (high-dimensional problems) to perform the *p-refinement* in higher dimensions ($d = 2,\, 3$), we choose the exact solution

$$u^{exact} = t^{p_1} \times \prod_{i=1}^{d} ((1+x_i)^{p_{2i}} - \epsilon(1+x)^{p_{2i+1}}), \tag{62}$$

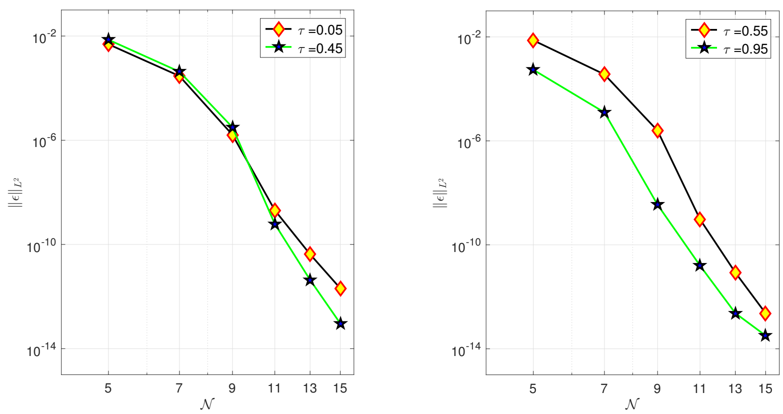

(a) (b)

Figure 1: Temporal *p-refinement*: log-log scale L^2-error versus temporal expansion orders $\mathcal{N}$ for test case (II).

where $p_1 = 7\frac{2}{3}$, $p_2 = 6\frac{1}{3}$, $p_3 = 6\frac{2}{7}$, $p_4 = 7\frac{4}{5}$, $p_5 = 7\frac{1}{7}$, $p_6 = 7\frac{3}{5}$, $p_7 = 7\frac{1}{7}$ and $\epsilon_1 = 2^{p_2-p_3}$, $\epsilon_2 = 2^{p_4-p_5}$, $\epsilon_3 = 2^{p_6-p_7}$ in the hypercube domain as $\underbrace{[0,\,1]\times[-1,\,1]\times\cdots\times[-1,\,1]}_{d\ times}$.

Test case (IV): (CPU time) to examine the efficiency of the method for the high-dimensional domain, we employ (62), where $p_1 = 4$, $p_{2i} = 3\frac{1}{3}$, $p_{2i} = 3\frac{2}{7}$, $\epsilon_i = 2^{p_{2i}-p_{2i+1}}$, $t \in [0,1]$, and $x \in [-1,1]^d$. In the following numerical examples, we illustrate the convergence rate and efficiency of the method, employing the test cases.

5.1. Numerical Test (I)

We plot the log-log scale L^2-error versus temporal orders $\mathcal{N}$ in Fig. 1 in a log-log scale plot for the test case (I) while $2\tau = \frac{1}{10}, \frac{9}{10}$, $2\mu_1 = \frac{5}{10}$, $2\nu_1 = \frac{15}{10}$, $T = 1$ and spatial expansion order is fixed ($\mathcal{M} = 23$). Having the same set-up, we also consider $2\tau = \frac{11}{10}, \frac{19}{10}$ in the temporal direction to examine the spectral convergence of fractional wave equation. The L^2-error decays linearly in the log-log scale plot as temporal expansion order $\mathcal{N}$ increases in both cases, indicating the spectral convergence of PG method. In [2], we obtain the theoretical convergence rate of $\|e\|_{L^2}$ and compare with the corresponding practical ones.

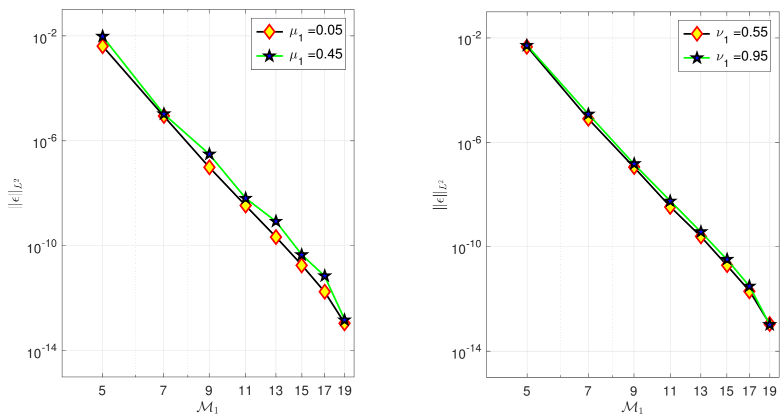

(a) (b)

Figure 2: Spatial *p-refinement*: log-log scale L^2-error versus spatial expansion orders $\mathcal{M}$ for the test case (II).

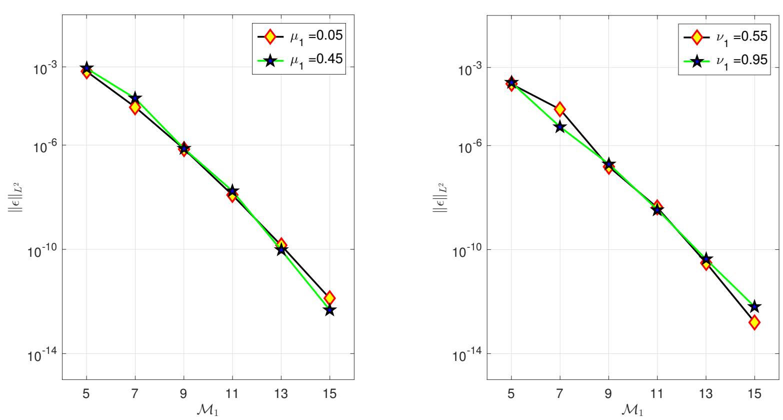

(a) (b)

Figure 3: Exponential convergence in the spatial *p-refinement*: log-log scale L^2-error versus spatial expansion orders $\mathcal{M}$ for the test case (I).

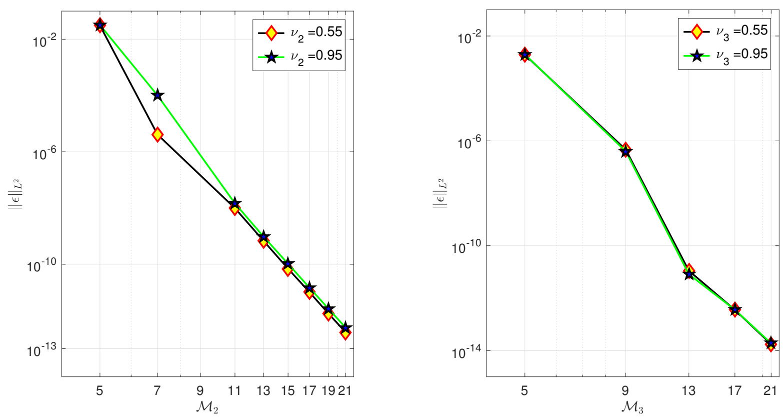

(a) (b)

Figure 4: Spatial *p-refinement*: log-log scale L^∞-error versus spatial expansion orders $\mathcal{M}_2$, $\mathcal{M}_3$ in the test case (III) for the limit fractional orders of ν.

5.2. Numerical Test (II)

Here, we perform the spatial *p-refinement* while the temporal expansion order is fixed for the test case (I). In Fig. 2, spectral convergence of log-log scale L^∞-error versus spatial expansion orders $\mathcal{M}_1$ is shown where $2\nu_1 = \frac{11}{10}$, $\frac{19}{10}$ in setup (a). We set $2\tau = \frac{6}{10}$, $2\mu_1 = \frac{5}{10}$, $T = 1$ and temporal expansion order is fixed ($\mathcal{N} = 23$). In this case, the limit fractional orders of ν_1 are examined, where both have the spectral convergence but with different rates. We also carried out the spatial *p-refinement* for the limit fractional orders of μ_1. The spectral convergence of the PG method is observed, where $2\mu_1 = \frac{1}{10}$, $\frac{9}{10}$ and $2\nu_1 = \frac{5}{10}$. To this end, we can conclude that the PG method in (1+1) dimensional space-time domain is spectrally accurate up to the order of 10^{-15}.

5.3. Numerical Test (III)

In Fig. 3, we plot $\|e\|_{L^2} = \|u - u^{ext}\|_{L^2}$ versus spatial expansion orders $\mathcal{M}$ for the test case (II), showing the spatial *p-refinement*. In setup (a) $2\nu_1 = \frac{11}{10}$, $\frac{19}{10}$ and $2\mu_1 = \frac{5}{10}$ and in setup (b) $2\mu_1 = \frac{11}{10}$, $\frac{19}{10}$ and $2\nu_1 = \frac{5}{10}$ where $2\tau = \frac{6}{10}$. The temporal expansion order ($\mathcal{N} = 23$) is fixed. The exponential convergence in the log-linear scale plot is illustrated clearly for the limit fractional orders of μ_1 and ν_1 in case spatial component of the exact solution is a sinusoidal smooth function.

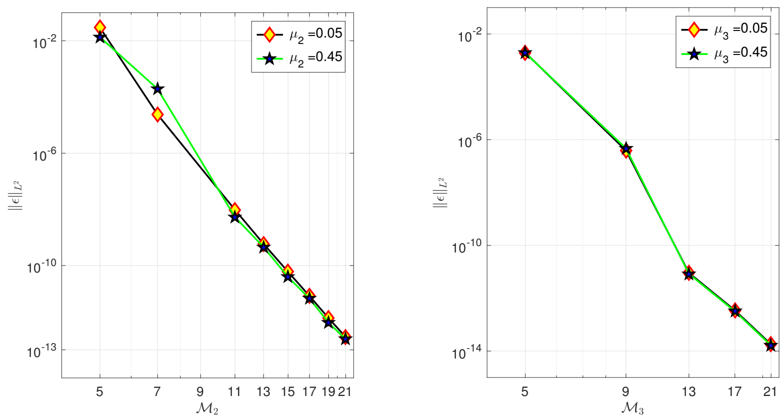

(a) (b)

Figure 5: Spatial *p-refinement*: log-log scale L^∞-error versus spatial expansion orders $\mathcal{M}_2$, $\mathcal{M}_3$ for the test case (III) for the limit fractional orders of μ.

5.4. Numerical Test (IV)

In addition to spatial/temporal *p-refinement*, we perform *p-refinement* for (1+2) and (1+3) as the higher dimensional domain in the test case (III). In Fig. 4, the spectral convergence of log-log L^∞-error versus spatial expansion orders $\mathcal{M}_2$, $\mathcal{M}_3$ is shown. In setup (a), $2\nu_2 = \frac{11}{10}$, $\frac{19}{10}$ while $2\nu_1 = \frac{15}{10}$, $2\mu_1 = \frac{4}{10}$ and $2\mu_2 = \frac{6}{10}$ and setup (b) $2\nu_3 = \frac{11}{10}$, $\frac{19}{10}$ while $2\nu_1 = \frac{14}{10}$, $2\nu_2 = \frac{16}{10}$, $2\mu_1 = \frac{3}{10}$, $2\mu_2 = \frac{5}{10}$ and $2\mu_3 = \frac{7}{10}$, where $2\tau = \frac{6}{10}$, $T = 1$. Furthermore, we increase the maximum bases order uniformly in all dimensions.

Similarly, we perform the spatial *p-refinement* for the limit fractional orders of μ in FADE. We study setup (a) $2\mu_2 = \frac{1}{10}$, $\frac{9}{10}$ while $2\mu_1 = \frac{5}{10}$, and setup (b) $2\mu_3 = \frac{1}{10}$, $\frac{9}{10}$ while $2\mu_1 = \frac{4}{10}$, $2\mu_2 = \frac{6}{10}$. In both setups, $2\tau = \frac{6}{10}$, $2\nu_1 = \frac{5}{10}$, $2\nu_2 = \frac{5}{10}$, $T = 1$. Furthermore, $\mathcal{N} = \mathcal{M}_1 = \mathcal{M}_2 = \mathcal{M}_3$ changes concurrently. In Fig. 5, the PG method shows spectral convergence for the limit fractional orders of μ.

5.5. Numerical Test (V)

To examine the efficiency of the PG method and the fast solver in high-dimensional problem, the convergence results and CPU time for test case (IV) are presented in Table 1 for (1+1), (1+3) and (1+5) dimensional space-time hypercube domains where the error is measured by the essential norm $\|e\|_\infty$ in the test case (IV). The CPU time is obtained on Intel (Xeon E52670)

Table 1: Performance study and CPU time (in sec.) of the unified PG spectral method for the test case (IV). In each step, we uniformly increase the bases order by one in all dimensions.

2-D FADRE

$\mathcal{N}$	$\Vert\epsilon\Vert_{L^\infty}$	CPU Time [Sec]
5	0.008	1.48
7	0.0003	3.01
9	1.69×10^{-6}	3.48
15	2.96×10^{-11}	4.95

3-D FADRE

$\mathcal{N}$	$\Vert\epsilon\Vert_{L^\infty}$	CPU Time [Sec]
5	0.01	1.43
7	0.0003	5.39
9	2.6×10^{-7}	6.14
15	2.41×10^{-10}	7.54

4-D FADRE

$\mathcal{N}$	$\Vert\epsilon\Vert_{L^\infty}$	CPU Time [Sec]
5	0.00005	3.56
7	3.31×10^{-7}	8.87
9	8.17×10^{-9}	5.37
15	9.70×10^{-12}	55.78

2.5 GHz processor. The presented PG method remains spectrally accurate in (1+5) dimensional time-space domain.

6. Summary and Discussion

6.1. Summary

We developed a new unified Petrov-Galerkin spectral method for a class of fractional partial differential equations with constant coefficients (14) in a $(1+d)$-dimensional *space-time* hypercube, $d = 1, 2, 3$, etc, subject to homogeneous Dirichlet initial/boundary conditions. We employed *Jacobi polyfractonomials*, as temporal basis/test functions, and the Legendre polynomials as spatial basis/test functions, yielding spatial mass matrices being independent of the spatial fractional orders. Additionally, we formulated the novel unified fast linear solver for the resulting high-dimensional linear system, which reduces the computational cost significantly. In fact, the main idea of the paper was to formulate a closed-form solution for the high-dimensional Lyapunov equation in terms of the eigensolutions up to the precision accuracy of computationally obtained eigensolutions. The PG method has been illustrated to be spectrally accurate for power-law test cases in each dimension. Furthermore, exponential convergence is observed for a sinusoidal smooth function in a spatial p-refinement. To check the stability and spectral convergence of the PG method, we carried out the corresponding discrete stability and error analysis of the method for (15) in [2].

Despite the high accuracy and the efficiency of the method especially in higher-dimensional problems, treatment of FPDEs in complex geometries and FPDEs with variable coefficients will be studies in our future works.

Appendix

Here, we provide the force function based on the exact solutions.

- ***Force term of test case (I)***

To obtain f in (14) based on (60), first we need to calculate all fractional derivatives of u^{ext}. To satisfy the corresponding boundary conditions, $\epsilon_i = 2^{p_{2i}-p_{2i+1}}$. Take $X^T = t^{p_1}$ and $X_i^S = (1+\zeta_i)^{p_{2i}} - \epsilon_i\,(1+\zeta_i)^{p_{2i+1}}$, where $\zeta_i = 2\frac{x_i-a_i}{b_i-a_i} - 1$ and $\zeta_i \in [-1\,,\,1]$. Considering (2),

$$ {}_0\mathcal{D}_t^{2\tau}\, X^T = \frac{\Gamma[p_1+1]}{\Gamma[p_1+1-2\tau]}\, t^{p_1-2\tau} = (\tfrac{T}{2})^{p_1-2\tau} \frac{\Gamma[p_1+1]}{\Gamma[p_1+1-2\tau]}\,(1+\eta(t))^{p_1-2\tau}, \qquad (63) $$

where $\eta(t) = 2(\frac{t}{T}) - 1$. Similarly,

$$
{}_{a_i}\mathcal{D}_{x_i}^{2\mu_i}\, X_i^S = \left(\frac{b_i-a_i}{2}\right)^{-2\mu_i}\Big[\frac{\Gamma[p_{2i}+1]}{\Gamma[p_{2i}+1-2\mu_i]}(1+\zeta_{2i}(x_i))^{p_{2i}-2\mu_i} - \epsilon_i \frac{\Gamma[p_{2i+1}+1]}{\Gamma[p_{2i+1}+1-2\mu_i]}(1+\zeta_{2i}(x_i))^{p_{2i+1}-2\mu_i}\Big], \tag{64}
$$

and

$$
{}_{a_i}\mathcal{D}_{x_i}^{2\nu_i}\, X_i^S = \left(\frac{b_i-a_i}{2}\right)^{-2\nu_i-2}\Big[\frac{\Gamma[p_{2i}+1]}{\Gamma[p_{2i}+1-2\nu_i]}(1+\zeta_{2i}(x_i))^{p_{2i}-2\nu_i} - \epsilon_i \frac{\Gamma[p_{2i+1}+1]}{\Gamma[p_{2i+1}+1-2\nu_i]}(1+\zeta_{2i}(x_i))^{p_{2i+1}-2\nu_i}\Big]. \tag{65}
$$

Therefore,

$$
\begin{aligned}
f &= (\frac{T}{2})^{p_1-2\tau}\frac{\Gamma[p_1+1]}{\Gamma[p_1+1-2\tau]}\,(1+\eta)^{p_1-2\tau}\prod_{i=1}^{d}(1+\zeta_i)^{p_{2i}} - \epsilon_i\,(1+\zeta_i)^{p_{2i+1}} \\
&+ \sum_{i=1}(\frac{T}{2})^{p_1}(1+\eta)^{p_1}\Big(c_{l_i}\,\Big(\frac{b_i-a_i}{2}\Big)^{-2\mu_i}\Big[\frac{\Gamma[p_{2i}+1]}{\Gamma[p_{2i}+1-2\mu_i]}(1+\zeta_{2i})^{p_{2i}-2\mu_i} \\
&- \epsilon_i\frac{\Gamma[p_{2i+1}+1]}{\Gamma[p_{2i+1}+1-2\mu_i]}(1+\zeta_{2i})^{p_{2i+1}-2\mu_i}\Big]\prod_{j=1,\,j\neq i}^{d}[(1+\zeta_j)^{p_{2j}} - \epsilon_j\,(1+\zeta_j)^{p_{2j+1}}]\Big) \\
&- \sum_{i=1}(\frac{T}{2})^{p_1}(1+\eta)^{p_1}\Big(\kappa_{l_i}\,\Big(\frac{b_i-a_i}{2}\Big)^{-2\nu_i-2}\Big[\frac{\Gamma[p_{2i}+1]}{\Gamma[p_{2i}+1-2\mu_i]}(1+\zeta_{2i})^{p_{2i}-2\nu_i} \\
&- \epsilon_i\frac{\Gamma[p_{2i+1}+1]}{\Gamma[p_{2i+1}+1-2\nu_i]}(1+\zeta_{2i})^{p_{2i+1}-2\nu_i}\Big]\prod_{j=1,\,j\neq i}^{d}[(1+\zeta_j)^{p_{2j}} - \epsilon_j\,(1+\zeta_j)^{p_{2j+1}}]\Big).
\end{aligned} \tag{66}
$$

- ***Force term of test case (II)***

  Take $X^T = t^{p_1}$ and $X_i^S = sin\big(n\pi\zeta\big)$. Here, we approximate X_i^S as

$$
X^S = \Sigma_{j=1}^{N_s}(-1)^{2j-1}\frac{(n\pi\zeta)^{2j-1}}{(2j-1)!}, \tag{67}
$$

where N_s controls the level of approximation error. Taking the same steps of (66), we obtain

$$\begin{aligned} f &= (\frac{T}{2})^{p_1-2\tau}\frac{\Gamma[p_1+1]}{\Gamma[p_1+1-2\tau]}(1+\eta)^{p_1-2\tau}\Sigma_{j=1}^{N_s}(-1)^{2j-1}\frac{(n\pi\zeta)^{2j-1}}{(2j-1)!} \\ &+ (\frac{T}{2})^{p_1}(1+\eta)^{p_1}\big[(c_l)\left(\frac{b-a}{2}\right)^{-2\mu}\Sigma_{j=1}^{N_s}(-1)^{2j-1}\frac{(n\pi\zeta)^{2j-1}}{(2j-1)!}\frac{\Gamma[2j]}{\Gamma[2j-2\mu]}\zeta^{2j-2\mu} \\ &- (\kappa_l)\left(\frac{b-a}{2}\right)^{-2\nu-2}\Sigma_{j=1}^{N_s}(-1)^{2j-1}\frac{(n\pi\zeta)^{2j-1}}{(2j-1)!}\frac{\Gamma[2j]}{\Gamma[2j-2\nu]}\zeta^{2j-2\nu}\big]. \end{aligned} \tag{68}$$

Acknowledgement

This work was supported by the MURI/ARO on Fractional PDEs for Conservation Laws and Beyond: Theory, Numerics and Applications (W911NF-15-1-0562).

References

[1] M. Zayernouri, G. E. Karniadakis, Fractional Sturm–Liouville eigen-problems: theory and numerical approximation, Journal of Computational Physics 252 (2013) 495–517.

[2] M. Samiee, M. Zayernouri, M. M. Meerschaert, A Unified Spectral Method for FPDEs with Two-sided Derivatives; part II: Stability and Error Analysis, submitted to Journal of Computational Physics, 2016 .

[3] I. Podlubny, Fractional differential equations: an introduction to fractional derivatives, fractional differential equations, to methods of their solution and some of their applications, vol. 198, Academic press, 1998.

[4] M. M. Meerschaert, A. Sikorskii, Stochastic models for fractional calculus, vol. 43, Walter de Gruyter, 2012.

[5] B. Guo, X. Pu, F. Huang, Fractional partial differential equations and their numerical solutions, World Scientific, 2015.

[6] S. G. Samko, A. A. Kilbas, O. I. Marichev, Fractional integrals and derivatives, Theory and Applications, Gordon and Breach, Yverdon 1993.

[7] A. Carpinteri, F. Mainardi, Fractals and fractional calculus in continuum mechanics, vol. 378, Springer, 2014.

[8] R. Klages, G. Radons, I. M. Sokolov, Anomalous Transport: Foundations and Applications, Wiley-VCH, 2008.

[9] R. Metzler, J. Klafter, The random walk's guide to anomalous diffusion: a fractional dynamics approach, Physics reports 339 (1) (2000) 1–77.

[10] G. M. Zaslavsky, J. Meiss, Physics of Chaos in Hamiltonian systems, Nature 398 (6725) (1999) 303.

[11] P. Perdikaris, G. E. Karniadakis, Fractional-order viscoelasticity in one-dimensional blood flow models, Annals of biomedical engineering 42 (5) (2014) 1012–1023.

[12] R. L. Magin, Fractional calculus in bioengineering, Begell House Redding, 2006.

[13] B. M. Regner, Randomness in Biological Transport .

[14] M. Naghibolhosseini, Estimation of outer-middle ear transmission using DPOAEs and fractional-order modeling of human middle ear, Ph.D. thesis, City University of New York, NY., 2015.

[15] T. Solomon, E. R. Weeks, H. L. Swinney, Observation of anomalous diffusion and Lévy flights in a two-dimensional rotating flow, Physical Review Letters 71 (24) (1993) 3975.

[16] T. Solomon, E. R. Weeks, H. L. Swinney, Chaotic advection in a two-dimensional flow: Lévy flights and anomalous diffusion, Physica D: Nonlinear Phenomena 76 (1) (1994) 70–84.

[17] M. M. Meerschaert, F. Sabzikar, M. S. Phanikumar, A. Zeleke, Tempered fractional time series model for turbulence in geophysical flows, Journal of Statistical Mechanics: Theory and Experiment 2014 (9) (2014) P09023.

[18] D. del Castillo-Negrete, B. Carreras, V. Lynch, Fractional diffusion in plasma turbulence, Physics of Plasmas (1994-present) 11 (8) (2004) 3854–3864.

[19] D. del Castillo-Negrete, P. Morrison, Chaotic transport by Rossby waves in shear flow, Physics of Fluids A: Fluid Dynamics (1989-1993) 5 (4) (1993) 948–965.

[20] D. A. Benson, R. Schumer, M. M. Meerschaert, S. W. Wheatcraft, Fractional dispersion, Lévy motion, and the MADE tracer tests, in: Dispersion in Heterogeneous Geological Formations, Springer, 211–240, 2001.

[21] D. A. Benson, S. W. Wheatcraft, M. M. Meerschaert, Application of a fractional advection-dispersion equation, Water Resources Research 36 (6) (2000) 1403–1412.

[22] K. Vafai, Handbook of porous media, Crc Press, 2015.

[23] F. Mainardi, Fractional calculus and waves in linear viscoelasticity: an introduction to mathematical models, World Scientific, 2010.

[24] C. Lubich, Discretized fractional calculus, SIAM Journal on Mathematical Analysis 17 (3) (1986) 704–719.

[25] N. Sugimoto, Burgers equation with a fractional derivative; hereditary effects on nonlinear acoustic waves, Journal of fluid mechanics 225 (1991) 631–653.

[26] N. Sugimoto, Generalized Burgers equations and fractional calculus, Nonlinear wave motion 408 (1989) 162–179.

[27] M. M. Meerschaert, C. Tadjeran, Finite difference approximations for fractional advection–dispersion flow equations, Journal of Computational and Applied Mathematics 172 (1) (2004) 65–77.

[28] C. Tadjeran, M. M. Meerschaert, A second-order accurate numerical method for the two-dimensional fractional diffusion equation, Journal of Computational Physics 220 (2) (2007) 813–823.

[29] H. Hejazi, T. Moroney, F. Liu, A finite volume method for solving the two-sided time-space fractional advection-dispersion equation, Open Physics 11 (10) (2013) 1275–1283.

[30] M. Chen, W. Deng, A second-order numerical method for two-dimensional two-sided space fractional convection diffusion equation, Applied Mathematical Modelling 38 (13) (2014) 3244–3259.

[31] F. Zeng, C. Li, F. Liu, I. Turner, Numerical algorithms for time-fractional subdiffusion equation with second-order accuracy, SIAM Journal on Scientific Computing 37 (1) (2015) A55–A78.

[32] X. Zhao, Z.-z. Sun, G. E. Karniadakis, Second-order approximations for variable order fractional derivatives: algorithms and applications, Journal of Computational Physics 293 (2015) 184–200.

[33] D. Li, C. Zhang, M. Ran, A linear finite difference scheme for generalized time fractional Burgers equation, Applied Mathematical Modelling .

[34] L. Feng, P. Zhuang, F. Liu, I. Turner, J. Li, High-order numerical methods for the Riesz space fractional advection–dispersion equations, Computers & Mathematics with Applications .

[35] F. Zeng, Z. Zhang, G. E. Karniadakis, Fast difference schemes for solving high-dimensional time-fractional subdiffusion equations, Journal of Computational Physics 307 (2016) 15–33.

[36] M. Zayernouri, A. Matzavinos, Fractional Adams–Bashforth/Moulton methods: An application to the fractional Keller–Segel chemotaxis system, Journal of Computational Physics 317 (2016) 1–14.

[37] J. Shen, L.-L. Wang, Fourierization of the Legendre–Galerkin method and a new space–time spectral method, Applied numerical mathematics 57 (5) (2007) 710–720.

[38] N. Sweilam, M. Khader, M. Adel, Chebyshev pseudo-spectral method for solving fractional advection-dispersion equation, Applied Mathematics 5 (19) (2014) 3240.

[39] F. Chen, Q. Xu, J. S. Hesthaven, A multi-domain spectral method for time-fractional differential equations, Journal of Computational Physics 293 (2015) 157–172.

[40] P. Mokhtary, Discrete Galerkin method for fractional integro-differential equations, arXiv preprint arXiv:1501.01111 .

[41] M. Zayernouri, M. Ainsworth, G. E. Karniadakis, Tempered Fractional Sturm–Liouville EigenProblems, SIAM Journal on Scientific Computing 37 (4) (2015) A1777–A1800.

[42] M. Zayernouri, G. E. Karniadakis, Spectral and discontinuous spectral element methods for fractional delay differential equations, Submitted to SIAM J. Scientific Computing .

[43] M. Zayernouri, G. E. Karniadakis, Exponentially accurate spectral and spectral element methods for fractional ODEs, Journal of Computational Physics 257 (2014) 460–480.

[44] M. Zayernouri, G. E. Karniadakis, Fractional spectral collocation method, SIAM Journal on Scientific Computing 36 (1) (2014) A40–A62.

[45] M. Zayernouri, M. Ainsworth, G. E. Karniadakis, A unified Petrov–Galerkin spectral method for fractional PDEs, Computer Methods in Applied Mechanics and Engineering 283 (2015) 1545–1569.

[46] M. Zayernouri, G. E. Karniadakis, Fractional spectral collocation methods for linear and nonlinear variable order FPDEs, Journal of Computational Physics 293 (2015) 312–338.

[47] M. Dehghan, M. Abbaszadeh, A. Mohebbi, Analysis of two methods based on Galerkin weak form for fractional diffusion-wave: Meshless interpolating element free Galerkin (IEFG) and finite element methods, Engineering Analysis with Boundary Elements 64 (2016) 205–221.

[48] M. Dehghan, M. Abbaszadeh, A. Mohebbi, The use of element free Galerkin method based on moving Kriging and radial point interpolation techniques for solving some types of Turing models, Engineering Analysis with Boundary Elements 62 (2016) 93–111.

[49] L. Zhao, W. Deng, J. S. Hesthaven, Spectral methods for tempered fractional differential equations, Mathematics of Computation ISSN 0025-5718.

[50] S. Chen, J. Shen, L.-L. Wang, Generalized Jacobi functions and their applications to fractional differential equations, Preprint on arXiv .

[51] Z. Mao, J. Shen, Efficient spectral–Galerkin methods for fractional partial differential equations with variable coefficients, Journal of Computational Physics 307 (2016) 243–261.

[52] J. F. R. Askey, Integral representations for Jacobi polynomials and some applications, Journal of Mathematical Analysis and Applications 26.

[53] G. J. Fix, J. P. Roop, Least squares finite-element solution of a fractional order two-point boundary value problem, Computers & Mathematics with Applications 48 (7) (2004) 1017–1033.

[54] B. Baeumer, T. Luks, M. M. Meerschaert, Space-time fractional Dirichlet problems, arXiv preprint arXiv:1604.06421 .

[55] Z.-Q. Chen, M. M. Meerschaert, E. Nane, Space–time fractional diffusion on bounded domains, Journal of Mathematical Analysis and Applications 393 (2) (2012) 479–488.